Acta. Chim. Asiana., 2025, 8(2), 733-742
e-ISSN/p-ISSN 2550-0503/2550-049x
Available online at: www.aca.unram.ac.id

RESEARCH PAPER

Physically activated corn cob carbon for congo red and methanil yellow removal

Faridatun Sholehah[*a], Rabiatul Adawiyah[a], and Bahrun[b]

[a] Study Program Chemistry Education, Faculty of Teacher Training and Science, Nggusuwaru University Bima, Jalan Piere Tendean, Bima City, Indonesia
[b] Research Centre for Chemistry, National Research and Innovation Agency (BRIN), Banten, 15314, Indonesia
[*]E-mail: ridhas801@gmail.com

DOI: 10.29303/aca.v8i2.272

Article info:

Received 21/09/2025

Revised 13/10/2025

Accepted 26/10/2025

Available online 29/11/2025

Abstract: The conversion of agricultural residues into sustainable adsorbents provides an environmentally responsible pathway for advanced wastewater treatment. In this work, physically activated carbon was synthesized from corncob, an abundant and underutilized agricultural byproduct, through carbon dioxide activation at elevated temperatures. Comprehensive characterization using BET surface area analysis, SEM-EDX, and FTIR confirmed the formation of a highly porous structure with abundant surface functional groups, favourable for dye adsorption. The adsorbent exhibited excellent performance in removing Congo Red (CR) and Metanil Yellow (MY), achieving maximum adsorption capacities of 59.88 mg/g and 30.47 mg/g, respectively. The Langmuir isotherm provides a good description of the equilibrium data, while the kinetic results follow the pseudo-second-order model, indicating that monolayer chemisorption is the dominant mechanism. These findings underscore the potential of corncob-derived activated carbon as a cost-effective, renewable, and high-performance material for sustainable wastewater remediation.

Keywords: Corncob, Activated carbon, Dye adsorption, Wastewater treatment, Sustainable adsorbent.

Citation: Sholehah, F, Adawiyah, R, & Bahrun, B. (2025). Physically activated corn cob carbon for congo red and metanil yellow removal. Acta Chimica Asiana, 8(2), 733–742. https://doi.org/10.29303/aca.v8i2.272

INTRODUCTION

Synthetic dyes are widely used in key industrial sectors, including textiles, food processing, leather tanning, and pharmaceuticals, leading to the discharge of substantial quantities of dye-laden effluents into aquatic environments. Among these, Congo Red (CR) and Metanil Yellow (MY) are widely applied anionic dyes recognized for their recalcitrance and high toxicity [1,2]. Their persistence in the environment, coupled with known carcinogenic and mutagenic properties, presents substantial risks to aquatic ecosystems and human health [3]. The structural stability and resistance of these dyes to biodegradation severely limit the effectiveness of conventional wastewater treatment technologies [2, 4], thereby underscoring the need for more effective and sustainable remediation approaches [5].

Adsorption has emerged as a principal strategy for dye removal, owing to its operational simplicity, efficiency, and broad applicability [1]. Activated carbon, attributable to its remarkable surface area and porosity, remains the gold standard adsorbent for organic pollutants [6]. However, the widespread application of commercial activated carbon is constrained by high production costs and the environmental footprint associated with non-renewable feedstocks and chemical activation methods. The development of alternative adsorbents based on sustainable sourcing and environmentally friendly synthesis routes has

thus gained considerable research momentum [3,7].

Lignocellulosic agricultural residues, widely available and inexpensive, offer attractive prospects as precursors for activated carbon production [8]. Their valorization not only addresses biomass waste management but also facilitates the production of cost-effective, high-efficiency adsorbents compatible with circular economy principles [7]. Corncob, predominantly generated in maize-producing regions such as Bima, West Nusa Tenggara, Indonesia, is typically discarded or subjected to open burning, causing environmental burdens. Harnessing this readily available residue for adsorbent synthesis represents a viable strategy to transform waste into functional materials for environmental remediation [8].

Physical activation using carbon dioxide or steam offers a cleaner alternative to chemical activation, thereby minimizing the use of hazardous substances and enhancing environmental compatibility [4]. This method enables the tuning of porosity and surface characteristics, which are essential for optimizing adsorption capacities toward complex organic contaminants. Moreover, physical activation processes align closely with the tenets of green chemistry and sustainable engineering, thereby supporting the wider adoption of large-scale and eco-safe water treatment systems [9,10].

Despite the extensively reported applications of corncob-derived activated carbon, notable knowledge gaps remain. Previous studies have predominantly focused on chemical activation and single-dye adsorption, with limited exploration of physically activated carbon and simultaneous removal of multiple environmentally relevant dyes [8]. Furthermore, the relationship between the physicochemical properties of the adsorbent and its adsorption mechanisms requires further elucidation, especially for region-specific biomass such as Bima corncob. The present study addresses these gaps by synthesizing physically activated carbon from Bima corncob via carbon dioxide activation and systematically evaluating its performance in the adsorption of CR and MY [10, 11]. Comprehensive equilibrium and kinetic analyses are conducted to elucidate the adsorption mechanisms, with a focus on the sustainability and scalability of the developed material as a viable solution for treating dye-laden wastewater [1,2].

MATERIALS AND METHODS

The materials used were corn cobs collected in Wawo District, Bima Regency, West Nusa Tenggara, Congo Red (CR) and Metanil Yellow (MY) dyes of analytical purity, and distilled water. The equipment used in this study included: chemical glassware to support the analysis, an analytical balance, a furnace, an oven, a magnetic stirrer, FTIR, BET, SEM, and Personal Protective Equipment.

Activated Carbon Preparation

Dried corncob pieces were carbonized in a tube furnace under a nitrogen atmosphere at 450°C for 2 hours. The resulting charcoal was then ground and sieved to a 100-mesh size. The charcoal was then physically activated by heating at 600°C for 1 hour under a continuous flow of carbon dioxide gas to develop porosity and surface functional groups [4,7]. The activated carbon samples were cooled to room temperature in a nitrogen atmosphere and stored in airtight containers for further analysis [9].

CharacterizationCharacterization of Activated Carbon

Surface morphology was examined using a scanning electron microscope (SEM) instrument equipped with EDX. The surface area and pore structure of the activated carbon were analyzed using the Brunauer–Emmett–Teller (BET) method, based on nitrogen adsorption–desorption isotherms. Functional groups on the adsorbent surface were identified using Fourier Transform Infrared (FTIR) spectroscopy in the 4000–400 cm^{-1} range [3,8].

Adsorption Experiments and Statistical Validation

For kinetic and equilibrium experiments, 0.25 g of activated carbon was mixed with 50 mL of dye solution at the desired concentrations in 100 mL Erlenmeyer flasks. For time variation studies, the contact time was varied at 5, 10, 15, 30, 45, 60, 90, and 120 minutes, while initial concentrations were adjusted from 30 mg L^{-1} to 150 mg L^{-1} for isotherm experiments. Each batch experiment was performed in triplicate to ensure the reliability of the data. Mean values and standard deviations were calculated, and error bars representing ±SD are included in all graphical data presentations. Statistical differences were analyzed using one-way ANOVA ($p<0.05$) to confirm experimental repeatability [12].

After adsorption, the samples were filtered through Whatman No. 42 filter paper. The residual dye concentration was determined using a UV–Vis spectrophotometer at λ_max = 496 nm for CR and 430 nm for MY. The adsorption capacity (q_e) was computed using the mass–balance relationship [11,12]:

$$q_e = \frac{(C_0 - C_e)V}{m}$$

Where C_0 and C_e (mg L^{-1}) are the initial and equilibrium dye concentrations, V (L) is the solution volume, and m (g) is the adsorbent mass.

Kinetic and Isotherm Data Analysis

Kinetic data were modelled using pseudo-first order (PFO) and pseudo-second order (PSO) equations by plotting $\ln(q_e - q_t)$ versus t for PFO and t/q_t versus t for PSO, respectively. The best-fitting model was selected based on the determination coefficient (R^2).

Equilibrium data were analyzed using the Langmuir and the Freundlich isotherm models. The Langmuir parameters (q_{max}, K_L) were derived from linear regression of C_e/q_e versus C_e, while the Freundlich constants (K_F, n) were obtained from the linear plot of $\log q_e$ versus $\log C_e$. The goodness of fit was evaluated using the R-squared coefficient (R^2). All statistical analyses and curve fitting were performed using OriginPro2023 software [12].

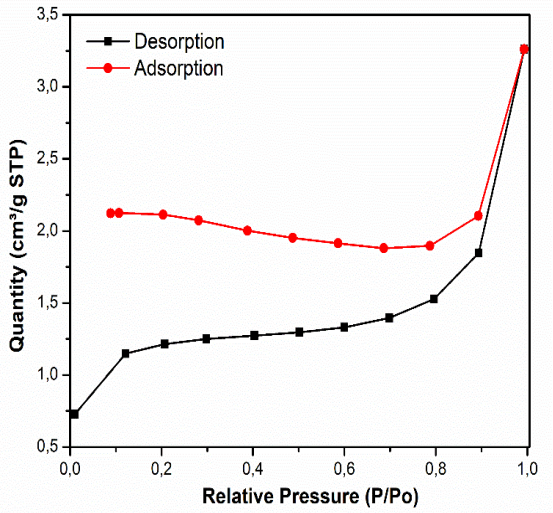

Figure 1. N2 adsorption/desorption isotherm of physically activated carbon

The physically activated carbon derived from corncob was characterized using the Brunauer–Emmett–Teller (BET) method, which revealed a specific surface area of 360.05 m²/g. The nitrogen adsorption-desorption isotherm is shown in Figure 1. The results show a typical type IV curve with a clear hysteresis loop at relative pressures (P/Po) above 0.4. This behaviour confirms the presence of mesopores within the material, indicating multilayer adsorption and capillary condensation mechanisms typical of mesoporous structures. The shape of the isotherm implies effective nitrogen uptake at intermediate to high relative pressures, reflecting the material's potential for high adsorption capacity.

Further analysis using the Barrett–Joyner–Halenda (BJH) method, derived from the nitrogen adsorption data, provided detailed insights into the pore size distribution. The pore volume and pore area distribution curves of BJH (Figure 2) show a predominance of medium-sized pores, with the cumulative pore volume and area decreasing sharply for pore radii above 40 Å. The average pore diameter was calculated to be 2.8026 nm (28.026 Å), which is within the mesoporous range as classified by the IUPAC standard. These structural characteristics highlight the suitability of activated carbon for applications involving mesoporous adsorption, with considerable potential for dye adsorption processes due to the predominance of mesoporous structures.

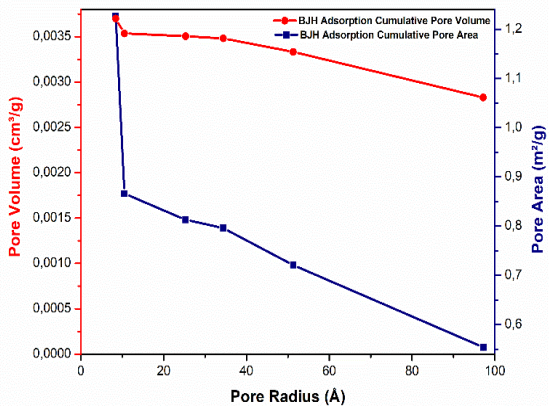

Figure 2. The pore volume and pore area distribution curves of the BJH of physically activated carbon

SEM images of physically activated corncob carbon at 5,000x (a) and 2,500x (b) magnifications reveal important microstructural features crucial for adsorption performance. At 5,000x magnification, the surface morphology exhibits irregular particle shapes with highly porous textures and visible micropores to mesoporosity, indicating the successful development of an extensive pore network that strongly supports high adsorption capacity. At 2,500x magnification, particle agglomerates

with interconnected pores become evident, forming a highly porous matrix that facilitates fluid transport and an effective adsorption mechanism [13]. Energy-dispersive X-ray spectroscopy (EDX) analysis further confirms the elemental composition and purity of the physically activated corncob carbon. These microstructural features collectively confirm the formation of a well-developed mesoporous structure, demonstrating the effectiveness of the physical activation process and showing promising potential for adsorption applications. The EDX spectrum results indicate that carbon is the dominant element, with a composition of 73.37% by weight, accompanied by significant iron (Fe) content of 22.61%, silicon (Si), and potassium (K) at 0.77% and 3.24%, respectively. The high carbon proportion reflects the effective carbonization and activation of the biomass.

Additionally, the presence of Fe is attributed to the corncob biomass, which is a common agricultural residue. Additionally, the presence of iron can also result from contamination during sample handling. The presence of this iron can contribute to introducing catalytic or functional properties of the surface, which have the potential to increase adsorption through redox interactions, resulting in increased adsorption sites for CR and MY dye adsorption [14].

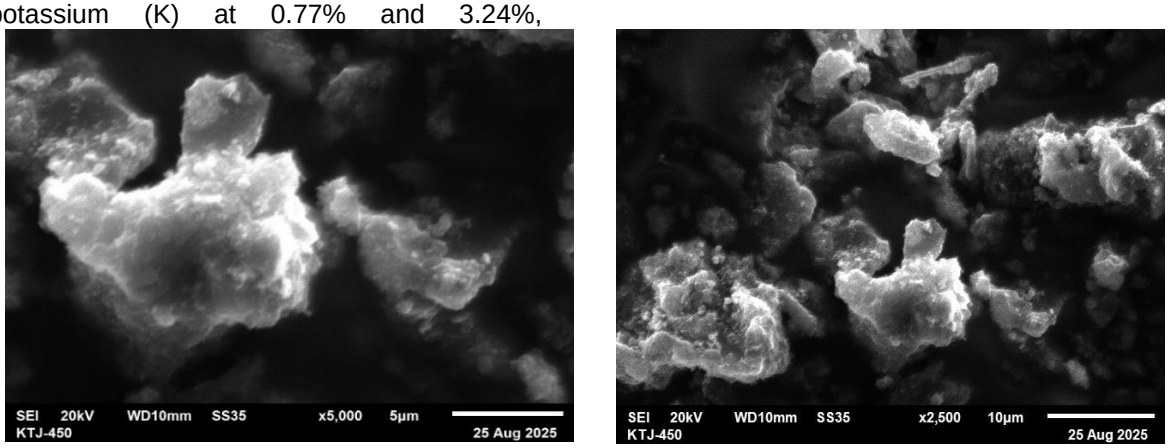

a b

Figure 3. Surface morphology of physically activated carbon with magnification (a) 5000x and (b) 2500x

The FTIR spectrum provides fundamental insights. Corncob-based activated carbon exhibits broad OH (~3400 cm^{-1}) and carbonyl (~1700 cm^{-1}) bands, indicating a high density of oxygenated surface functionalities. These groups enhance the material's hydrophilicity and provide diverse active sites for dye adsorption. The aromatic C=C stretching band (~1600 cm^{-1}) indicates the presence of graphitic domains, which may facilitate π–π bonding with aromatic dye molecules, thus enhancing dye adsorption through various types of interactions [15].

For methanil yellow, the presence of distinct absorption bands for azo (–N=N–, 1440–1506 cm^{-1}) and sulfonic ($–SO_3$, 1057–1041 cm^{-1}) groups confirms its anionic character and suggests favourable interaction mechanisms on the carbon surface, primarily through electrostatic attraction and hydrogen bonding. The broad hydroxyl and amine stretching observed at 3675–3500 cm^{-1} further supports the availability of polar groups. In CR dyes, azo (1446 cm^{-1}), sulfonic (1062 cm^{-1}), and carboxylic (1382 cm^{-1}, 1646 cm^{-1}) groups are present, confirming diverse binding sites. The broad NH/OH stretching at ~3460 cm^{-1} allows strong hydrogen bonding with the hydroxyl groups on the activated carbon surface. The presence of negatively charged and aromatic groups in CR further supports multi-point interactions, thus enhancing its adsorption by activated carbon. Overall, these findings suggest that physically activated corncob carbon facilitates efficient multimodal adsorption, driven by hydrogen bonding, π–π stacking, and electrostatic interactions. This combination of mechanisms enhances the material's effectiveness in removing aromatic azo dyes [16,17].

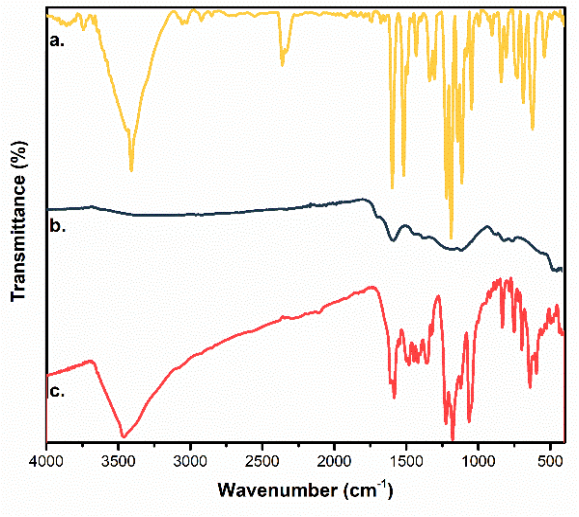

Figure 4. FTIR spectrum of a) MY dye, b) Physically activated carbon, c) CR dye.

Table 1. FTIR Analysis Results

Sample	Wavenumber (cm^{-1})	Functional Group
MY Dye	3675–3500	OH, NH
	1440–1506	N=N (Azo)
	1350–1180	CN
	1057–1041	S=O (Sulfonate)
Physically activated carbon	3400	-OH
	1700	C=O (Carbonyl)
	1100–1000	C-O
	1600	C=C (Aromatic)
CR Dye	3460	NH, OH (Hydrogen-Bonded)
	1646	C=C (Aromatic), COO-
	1446	N=N (Azo)
	1382	COO- (Symmetrical stretching)
	1062	S=O (Sulfonate)

Optimum Adsorption Time

The optimum adsorption time for physically activated carbon is shown in Figure 5. The results showed that CR reached adsorption capacity in approximately 30 minutes, while MY reached equilibrium in approximately 45 minutes. The shorter optimum time for Congo Red can be attributed to its larger molecular size and multifunctional groups, which facilitate rapid and strong interactions such as electrostatic attraction, hydrogen bonding, and π–π stacking with the activated carbon surface. These interactions allow for faster surface adsorption and saturation of active sites.

MY dye, which has a smaller and simpler molecular structure, exhibited a slower adsorption rate, requiring a longer contact time to diffuse into the carbon pores and fully occupy the available binding sites. This slower process is potentially due to fewer interaction points and less steric hindrance, which affect adsorption dynamics.

Experimental data indicate that both dyes better fit the pseudo-second-order kinetic model, as evidenced by higher correlation coefficients (R^2 approaching 1) and better agreement between calculated and experimental qe values. It suggests that the adsorption mechanism is primarily controlled by chemisorption, which involves the sharing

or exchange of electrons between dye molecules and active sites on the activated carbon surface. The higher PSO rate constant (k^2) for CR compared to MY indicates faster adsorption kinetics, likely due to the stronger interaction affinity and larger molecular size, which facilitates multivalent bonding. Overall, the kinetic analysis reveals a superior adsorption capacity and rate, attributed to the molecular complexity and potential interaction with physically activated carbon, which facilitates easier adsorption in a shorter time, as indicated by pseudo-second-order kinetics [20].

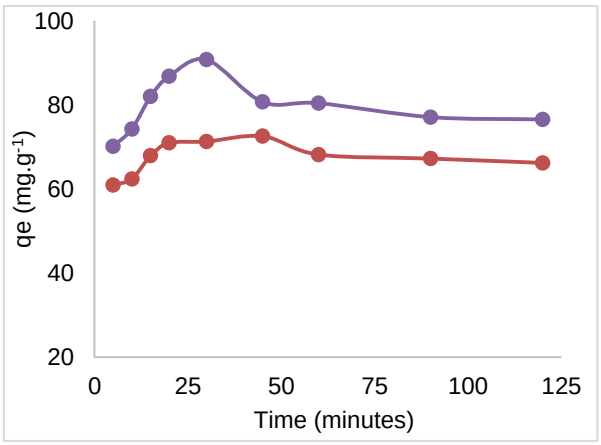

Figure 5. Effect of Carbon Contact Time on Dye a) CR b) MY

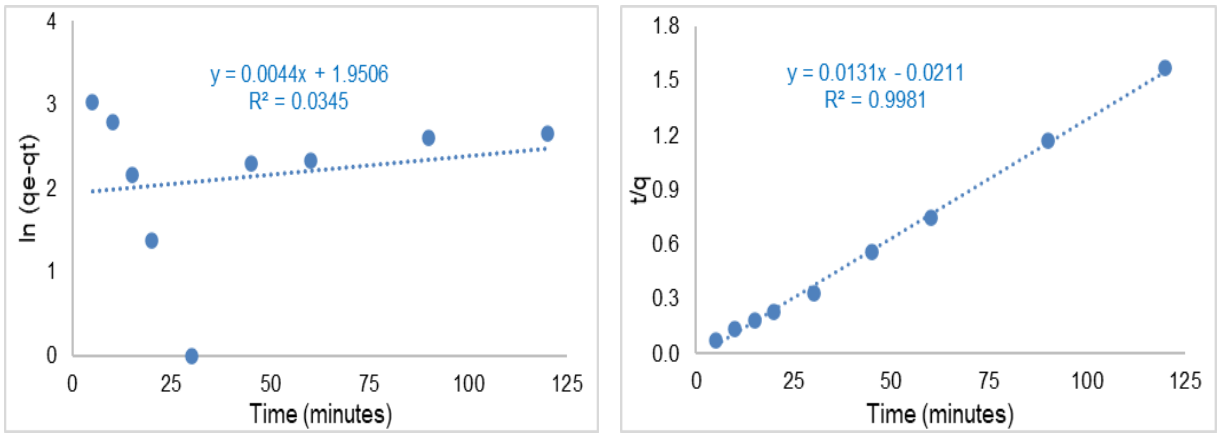

a b

Figure 6. Kinetic curves of Congo Red dye adsorption: a) pseudo-first-order, b) pseudo-second-order

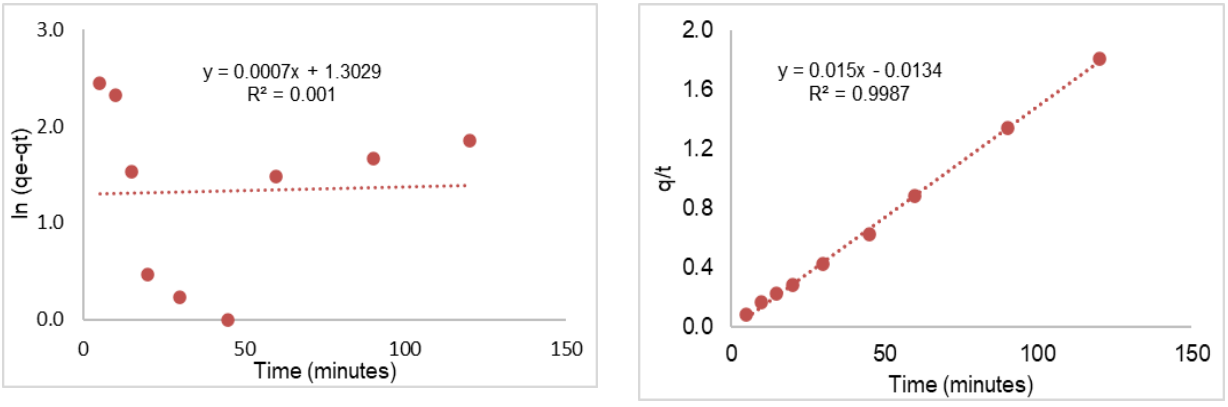

a b

Figure 7. Kinetic curves of Metanil Yellow dye adsorption: a) pseudo-first-order, b) pseudo-second-order

Table 2. Adsorption kinetic parameters for CR and MY on physically activated carbon.

	Pseudo first order			Pseudo-second order		
	qe (mg·g⁻¹)	K1	R2	qe (mg·g⁻¹)	K2	R2
CR	7.03	0.0044	0.0345	76.33	0.0081	0.9981
MY	3.68	0.0007	0.001	66.66	0.0167	0.9987

Batch experiment of dye adsorption

Figure 8 presents the adsorption isotherms of Congo Red (CR) and Metanil Yellow (MY) on physically activated corncob carbon, including the effect of equilibrium concentration (Ce) on adsorption capacity (qe), as well as a linear fit to the Langmuir and the Freundlich isotherm models. The plot in (Figure 8a) shows a consistent increase in adsorption capacity with increasing Ce for both dyes, with CR exhibiting a significantly higher qe compared to MY at all concentrations. This superior adsorption performance toward CR indicates a stronger interaction or greater affinity between the activated carbon surface and the CR molecules, likely due to molecular size, structure, or electrostatic interactions [21]

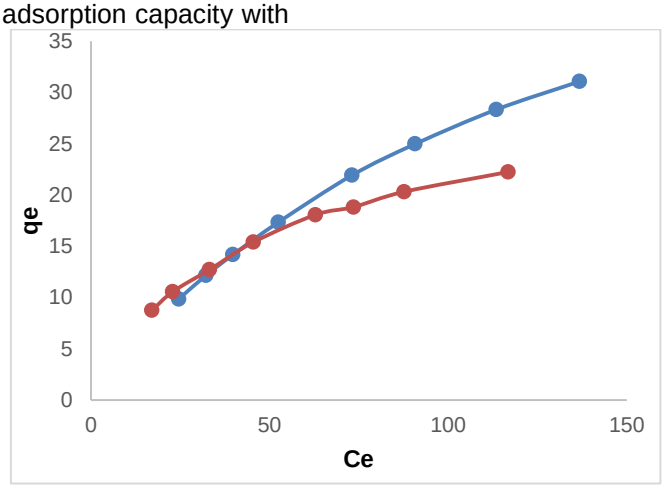

a

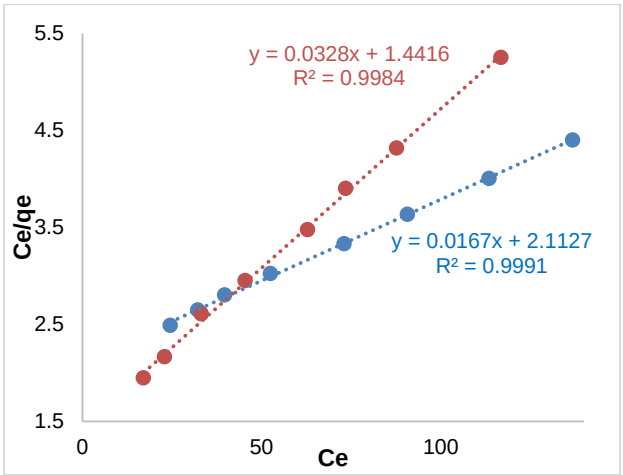

b

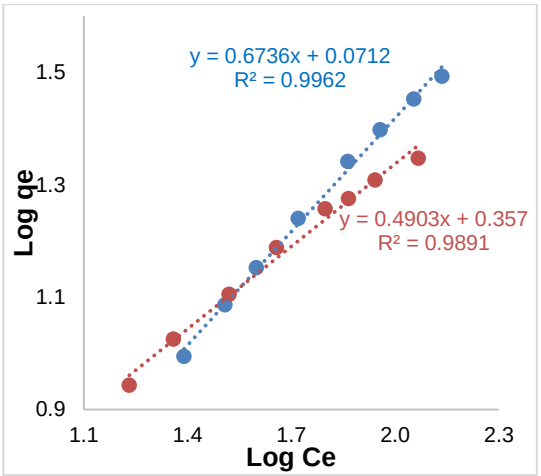

c

Figure 8. a) Effect of concentration of physically activated carbon, b) Langmuir isotherm, c) Freundlich isotherm

The Langmuir isotherm plot (Figure 8b) shows excellent linearity, with correlation coefficients (R^2) of 0.9984 for MY and 0.9991 for CR. CR exhibits monolayer adsorption on a homogeneous surface, consistent with a chemisorption mechanism. The high R^2 values confirm the goodness-of-fit of the Langmuir model, implying that physically activated corncob carbon has a uniform distribution of active sites, allowing for efficient and predictable adsorption (Sanwijaya et al., 2024). The higher slope for MY indicates a

slightly greater increase in adsorption sites with Ce, but the higher intercept for CR underscores its significantly greater adsorption capacity [15].

For the Freundlich isotherm (Figure 8c), the linear fit is again strong for both dyes, with R^2 values of 0.9962 for CR and 0.9891 for MY, indicating favourable multilayer adsorption on heterogeneous surfaces. Although the Freundlich model fits reasonably well, the superior fit of the Langmuir model, as evidenced by the higher R^2 values, indicates that monolayer adsorption dominates under the experimental conditions.

Table 3. Adsorption of the Congo Red and metanil yellow dye using various types of adsorbents

Adsorbent Type	**Dye**	**Maximum Adsorption Capacity, q_m (mg/g)**	**Reference**
Physically activated corncob carbon (this study)	Congo Red	59.88	Present study
Physically activated corncob carbon (this study)	Metanil Yellow	30.47	Present study
Chemically activated corncob carbon	Congo Red	53.76	[18]
Water hyacinth leaf adsorbent	Metanil Yellow	48.10	[20]
Reagent NiO	Congo Red	39.7	[22]
Cellulose from sago fround	Congo Red	15.63	[23]
Brewer's spent grain	Congo Red	36.5	[24]
Kawista fruit shells waste	Metanil Yellow	5,48	[25]
Corbicula moltkiana	Metanil Yellow	2,591	[26]

Comparison of various adsorbents Table 3 compares the adsorption capacities of various adsorbents used to remove CR and MY dyes. The most important parameter to compare is the Langmuir Qo value, as it measures the adsorption capacity of the adsorbent. The study reported superior adsorption capacities (59.88 mg/g for CR and 30.47 mg/g for MY) compared to many other biomass-derived adsorbents. These values demonstrate the high efficacy of physically activated corncob carbon in capturing CO_2 without the need for chemical activation. Some chemically activated or optimized carbons exhibit slightly higher or comparable adsorption capacities than CR and MY, but often involve more complex and less environmentally friendly processes. Mechanistic insights from the FTIR and kinetic modelling of the study, as well as the fit of the Langmuir isotherm model, support chemisorption driven by surface functional groups such as hydroxyl and carboxyl groups in this study. It positions your adsorbent as a cost-effective, sustainable, and high-performance candidate for treating dye-contaminated wastewater.

CONCLUSION

This study demonstrates the successful conversion of corncob agricultural waste into activated carbon through a continuous physical activation process using carbon dioxide at high temperatures. The synthesized activated carbon exhibits a highly porous structure, as confirmed by BET surface area analysis, SEM-EDX, and FTIR characterization, which provides numerous active sites and abundant functional groups conducive to the efficient adsorption of anionic dyes, specifically Congo Red (CR) and Metanil Yellow (MY). Maximum adsorption capacities of 59.88 mg/g for CR and 30.47 mg/g for MY were achieved. It's demonstrating competitive performance compared to other corncob-based adsorbents reported in the literature, which often involve chemical activation or more complex treatment procedures.

Thermodynamic analyses indicated that the adsorption process is spontaneous and endothermic, consistent with chemisorption mechanisms supported by pseudo-second-order kinetics and Langmuir isotherm modelling, implying monolayer dye uptake on homogeneous active sites. This study makes a valuable contribution to the advancement of green adsorbent synthesis by utilizing an abundant, cost-effective agricultural residue and employing a scalable, environmentally friendly activation method. The findings support the potential integration of corncob-based physically activated carbon in sustainable wastewater treatment technologies to mitigate dye pollution from textile and related industries, aligning with circular economy principles.

Acknowledgements

Thanks are extended to the Ministry of Education, Culture, Research, and Technology (Kemendikbudristek) of the Republic of Indonesia for the grant for Superior Basic Research in Higher Education (PDP) that supported this research. The authors also express their gratitude to the research facilities, as well as the scientific and technical support from the Lampung Advanced Characterisation Laboratory and the Advanced Nuclear Materials Laboratory of the BRIN National Research and Innovation Agency. They also extend their deepest gratitude to all parties who played a role in the implementation of the research.

REFERENCES

[1] Islam, M. M., Aidid, A. R., Mohshin, J. N., Mondal, H., Ganguli, S., & Chakraborty, A. K. (2025). A critical review on textile dye-containing wastewater: Ecotoxicity, health risks, and remediation strategies for environmental safety. *Cleaner Chemical Engineering*, 100165.

[2] Zainudin, N. F., Sam, S. T., Wong, Y. S., Ismail, H., Walli, S., Inoue, K., ... & Tan, W. K. (2023). Degradation of diazo Congo red dye by using synthesized poly-ferric-silicate-sulphate through Co-polymerization process. *Polymers*, *15*(1), 237.

[3] Putri, N. P., Riska, A. M., Kusumawati, D. H., & Suaebah, E. (2025). Enhanced Photocatalytic Degradation of Congo Red Dye Using Green-Synthesized TiO_2 and PANI/TiO_2 with Papaya Leaf as Bio-Reduction. *Trends in Sciences*, *22*(2), 9119-9119.

[4] Yahia, Y., Rashid, K. T., Shehab, M. A., Razak, A. A. A., Ghadhban, M. Y., Al-Lami, M., ... & Mahmood, A. (2025). Treating wastewater contaminated with congo red (CR) dye using an optimized polyethersulfone/propolis (bee glue) PES/PRS ultrafiltration membrane. *RSC advances*, *15*(29), 23174.

[5] Strebel, A., Behringer, M., Hilbig, H., Machner, A., & Helmreich, B. (2024). Anionic azo dyes and their removal from textile wastewater through adsorption by various adsorbents: a critical review. *Frontiers in Environmental Engineering*, *3*, 1347981.

[6] Yang, N., Ma, J., Shi, J., Yang, X., & Lu, J. (2022). Manipulate the nano-structure of layered double hydroxides via calcination for enhancing immobilization of anionic dyes on collagen fibers. *Journal of Colloid and Interface Science*, *610*, 182-193.

[7] Hendronursito, Y., Astuti, W., Sabarman, H., & Santoso, I. (2025). A porous activated carbon derived from banana peel by hydrothermal activation two-step methods. *International Journal of Renewable Energy Development*, *14*(2), 322-331.

[8] Zhang, N., Wang, F., Nwamba, M. C., Wang, D., & Hong, J. (2023). Enhancing tolerance of Kluyveromyces marxianus to lignocellulose-derived inhibitors and its ethanol production from corn cob via overexpression of a nitroreductase gene. *Industrial Crops and Products*, *203*, 117136.

[9] Sun, W., Liu, C., Liu, S., Zhang, J., Chen, H., & Qiu, Z. (2025). Effective adsorption of Congo red by an innovative biochar/LDH-derived MIL-100 (Al): Investigation of coexisting pollutants and mechanism revelation. *Separation and Purification Technology*, *359*, 130670.

[10] Al-Lami, H. S., Abdulwahid, A. A., & Mizhir, A. A. (2022). Adsorption process for removing hazardous Congo red dye from aqueous solutions: isotherm, kinetic, and thermodynamic studies. *Desalination and Water Treatment*, *280*, 177-187.

[11] Kulkarni, K., Kumar, P. M., Kulkarni, A., & Satpute, S. (2024). Bioremediation of hazardous Metanil yellow dye by using Trichoderma and Azotobacter biofertilizers. *Ecological Frontiers*, *44*(3), 605-617.

[12] Sholehah, F., Taba, P., Hala, Y., & Bahrun. (2021, September). Adsorption of congo red dyes using mesoporous silica MCM-48. In *AIP Conference Proceedings* (Vol. 2360, No. 1, p. 050013). AIP Publishing LLC.

[13] He, X., Chen, X., Wang, X., & Jiang, L. (2023). Optimization of activated carbon production from corn cob using

response surface methodology. *Frontiers in Environmental Science*, *11*, 1105408.

[14] Hamed, S. M., Samir, N., Atrees, M., & Abdelbasier, A. M. (2025). Kinetic Pathways for Uranium Adsorption from Contaminated Wastewater Using Activated Carbon Derived from Corn Cob as a Biosorbent. *Egyptian Journal of Chemistry*, *68*(11), 25-40. Doi

[15] Akande, J. A., Adeogun, A. I., & Uzosike, A. S. (2023). Removal of congo red dye from simulated wastewater using activated carbon derived from corn cobs; kinetics and equilibrium studies. *Glob J Pure Appl Chem Res*, *11*, 1-19. https://doi.org/10.37745/gjpacr.2023/vol 11n1119.

[16] Raghavendra, N., Hublikar, L. V., Sowmyashree, A. S., Nandan, K. R., Tubaki, A. B., Madiwalar, S. S., & Pudakalkatti, S. M. (2025). Fabrication of agro–waste corn cob–derived adsorbent for effective removal of oxalic acid from water: Pollution reducing and energy saving strategy for the wastewater treatment. *Next Materials*, *8*, 100844.

[17] Ojedokun, A. T., & Bello, O. S. (2017). Liquid phase adsorption of Congo red dye on functionalized corn cobs. *Journal of Dispersion Science and Technology*, *38*(9), 1285-1294.

[18] Sime, T., Fito, J., Nkambule, T. T., Temesgen, Y., & Sergawie, A. (2023). Adsorption of Congo red from textile wastewater using activated carbon developed from corn cobs: the studies of isotherms and kinetics. *Chemistry Africa*, *6*(2), 667-682.

[19] Zein, R., Chaidir, Z., Zilfa, Z., Fauzia, S., & Ramadhani, P. (2022). Isotherm and kinetic studies on the adsorption behavior of metanil yellow dyes onto modified shrimp shell-polyethylenimine (SS-PEI). *Jurnal Kimia Valensi*, *8*(1), 10-22.

[20] Aranda-García, E., Guerrero-Coronilla, I., & Cristiani-Urbina, E. (2024). Water Hyacinth Leaves Are an Efficient, Green, and Cost-Effective Biosorbent for the Removal of Metanil Yellow from Aqueous Solution: Kinetics, Isotherm, and Thermodynamic tudies. *Molecules*, *29*(14), 3409.

[21] Malviya, A., Jaspal, D. K., & Khamparia, S. (2019). Kinetics studies on the adsorption of Methyl Orange and Metanil Yellow onto bottom ash: a comparative account. *Water Science and Technology*, *80*(10), 1844-1850.

[22] Cheng, B., Le, Y., Cai, W., & Yu, J. (2011). Synthesis of hierarchical Ni (OH) 2 and NiO nanosheets and their adsorption kinetics and isotherms to Congo red in water. *Journal of hazardous materials*, *185*(2-3), 889-897.

[23] Arnata, I. W., Suprihatin, S., Fahma, F., Richana, N., & Sunarti, T. C. (2019). Adsorption of anionic congo red dye by using cellulose from sago frond. *Poll Res*, *38*(3), 43-53.

[24] Chanzu, H. A., Onyari, J. M., & Shiundu, P. M. (2019). Brewers' spent grain in adsorption of aqueous Congo Red and malachite Green dyes: Batch and continuous flow systems. *Journal of hazardous materials*, *380*, 120897.

[25] Santra, A. K., Pal, T. K., & Datta, S. (2008). Removal of metanil yellow from its aqueous solution by fly ash and activated carbon produced from different sources. Separation Science and Technology, 43(6), 1434-1458.

[26] R Mittal, A., Gupta, V. K., Malviya, A., & Mittal, J. (2008). Process development for the batch and bulk removal and recovery of a hazardous, water-soluble azo dye (Metanil Yellow) by adsorption over waste materials (Bottom Ash and De-Oiled Soya). Journal of Hazardous Materials, 151(2-3), 821-832.